ANGLE-PRESERVING MAPPINGS FOR THE VISUALIZATION OF MULTI-BRANCHED VESSELS

Lei Zhu, Steven Haker, Allen Tannenbaum

Georgia Institute of Technology
Department of Biomedical Engineering
Atlanta, GA 30332

Sylvain Bouix, Kaleem Siddiqi

McGill University
School of Computer Science
Montreal, QC H3A 2A7, Canada

ABSTRACT

In this note, we employ a conformal mapping technique to flatten tubular structures with multi-branches for visualization of MRA and CT volumetric vessel imagery. This may be used for the study of possible vessel pathology or virtual colonscopy for polyp detection. The method is based on a discrete Laplace-Beltrami operator to flatten a tubular surface onto a planar polygonal region in an angle-preserving manner. In this method, a thinned prunned medial surface (or skeleton) is used for the vessel partition.

Keywords: flattening maps, skeleton, conformal mappings, MRA brain imagery

1. INTRODUCTION

Recently, there has been some interest in various techniques for surface deformations, and in particular, the flattening of highly undulated and branched surfaces. For example, flattened representations of the brain surface are very important in applications such as functional magnetic resonance imaging by showing the details of neural activities within the folds of brain surface. A conformal mapping method is proposed in [4] in the context of virtual colonscopy for polyp detection. In [5], Y-shaped vessels are flattened in a similar way to give a clear representation of several geometric surface characteristics such as the mean curvature and Gaussian curvature. In this note, we consider the flattening of vessels with multiple branches. The applications of this method include lung nodule detection and coronary vessel stenosis from CT imagery as well as the detection of pathologies such as thrombosis in MRA brain imagery.

In [5], we formulated the algorithm of defining a cut on the vessel surface with a single branch. In this note, we will show how to extent this method to the flattening of multiply branched tubes. The key points include how to cut the whole vessel into segments and how to define appropriate boundary conditions.

We now outline the contents of this note. In Section 2, we give an overview of the flattening method. In Section 3, we summarize the use of skeletons to cut the surface and the determination of boundary conditions. Then in Section 4, we describe the numerical method employed for constructing the flattening map based on finite elements. Next in Section 5, we apply it to some MRA brain vessel imagery. Finally in Section 6, we discuss some possible future research directions.

2. APPROACH TO VESSEL FLATTENING

In this section, we will give an outline of our approach for the conformal flattening of a Y-shaped tubular structure (i.e., with only one branch point). The basic theory of Riemann surfaces can be found in [3], and the relevant results of partial differential equations can be found in [10].

Assume $\Sigma \subset \mathbf{R}^3$ represents an embedded surface (no self-intersections), which is topologically a tube with two tubular branches (see Figure 1). The tube has three boundaries, which are circles in topology. The boundaries are named as σ_0, σ_1 and σ_2, respectively. We want to construct a conformal map [9], $f : \Sigma \to \mathbf{C}$, which maps Σ to a planar polygonal-shaped region.

The first step of the construction of f is to solve a Dirichlet problem $\Delta u = 0$ on $\Sigma \backslash (\sigma_0 \cup \sigma_1 \cup \sigma_2)$. The boundary conditions should be chosen properly to guarantee that the branch point x_0 ($u'(x_0) = 0$) be located where the two branch tubes meet.

We then define three smooth curves C_0, C_1 and C_2 running from x_0 to σ_0, σ_1, and σ_2, respectively (see Figure 1), and such that these curves are along the gradient direction or opposite direction to the gradient of u. The curve C_i meets the boundary σ_i at point $y_i (i = 0, 1, 2)$. Since $u'(x_0) = 0$, we can make C_1 and C_2 lie on a line in a neighborhood of x_0, while C_0 is perpendicular to the line.

These curves define a cut on Σ. The cut and the original boundaries define an oriented boundary B of the cut surface:

$$y_0 \xrightarrow{\sigma_0} y_0 \xrightarrow{-C_0} x_0 \xrightarrow{C_1} y_1 \xrightarrow{\sigma_1} y_1 \xrightarrow{-C_1} x_0 \xrightarrow{C_2} y_2 \xrightarrow{\sigma_2} y_2 \xrightarrow{-C_2} x_0 \xrightarrow{C_0} y_0$$

where $-C_i$ means running the boundary in the opposite direction of C_i.

The second step of constructing the mapping function is to calculate the harmonic conjugate to u by solving another Dirichlet problem $\Delta v = 0$, given the boundary values of v satisfy

$$v(\zeta) = \int_{\zeta_0}^{\zeta} \frac{\partial v}{\partial s} ds = \int_{\zeta_0}^{\zeta} \frac{\partial u}{\partial n} ds \tag{1}$$

The proof that the mapping is one-to-one can be found in [9].

3. SKELETON AND BOUNDARY CONDITIONS

In this section, we will show how to use the skeleton to divide a multiply branched vessel into several parts in order to set the proper boundary conditions for the flattening. See [6] for an extensive list of references about the skeleton.

The skeleton of a closed set $A \subset \mathbf{R}^3$ is the locus of centers of maximal open balls contained within the set. Interest in the skeleton lies in the fact that it provides a complete and compact representation of an object, and contains both local (e.g. local width) and global information (e.g. number of holes) about the shape. $2D$ skeletons have been widely used in numerous applications such as object segmentation or generic object recognition and classification. $3D$ skeletons, also called medial surfaces, are becoming an important tool in computer vision especially in medical imaging, for segmentation, registration and statistical shape analysis.

We provide only a brief overview of our vessel tree extraction procedure here; full details will be published in the full version of this paper. The medial surface of the vessel data was generated by the method described in [6]. The key idea is to measure the average outward flux of the gradient of the distance transform of the object, and to detect locations where this flux is negative. This is done in conjunction with a topological thinning procedure in order to obtain thin and topologically correct medial surfaces. The medial surface is further thinned and pruned to generate a $3D$ curve with branches as shown in Figure 2.

The resulting curve is then segmented into curve points, branch points (marked by a blue star) and end points (marked by a red star). One of the end points is arbitrarily set to be the *root* and the other end points to be *leaves*. The *root* is assigned a value 0 and the value of a *leaf* is determined by the length of the curve from it to the *root*. These values are taken to be the boundary values in solving the Laplace equation for the harmonic function u as described in the previous section. Finally, the "vessel tree" is cut into several segments, each containing a Y-shaped structure. By using this partitioned skeleton as a reference, we can easily divide the whole vessel into several parts, each having only one branch point.

4. NUMERICAL METHOD FOR FLATTENING

In the previous section, we have partitioned the whole vessel into parts, each topologically being a Y-shaped tube. Here we will summarize the numerical approximation for the mapping function of each part using a finite element method [7]. More details can be found in [5]. In [1] and [4] we described related methods for brain flattening and colon flattening, respectively. The method used for vessel flattening is similar to them. However, due to the differences in topology, the boundary conditions have to be changed.

In this section, we assume that Σ is a triangulated surface. Let $PL(\Sigma)$ denote the finite dimensional space of piecewise linear functions on Σ. Then we define a basis $\{\phi_V\}$ for $PL(\Sigma)$. For each vertex, there is a corresponding piecewise linear basis function which is 1 on this vertex and 0 on all other vertices, i.e.

$$\begin{aligned} &\phi_V(V) &&= 1, \\ &\phi_V(W) &&= 0,\ W \neq V, \\ &\phi_V \text{ is linear on each triangle.} \end{aligned} \tag{2}$$

Any function $u \in PL(\Sigma)$ can be approximated as the linear combination of these basis functions. The coefficients are the values on vertices:

$$u = \sum_V u_V \phi_V. \tag{3}$$

What we are looking for is a flattening function f that is continuous on Σ and piecewise linear on each triangle. It is known [10] that the solution to the Laplace function $\Delta u = 0$ is the harmonic function u which minimizes the Dirichlet functional

$$D(u) = \frac{1}{2} \int \int_{\Sigma} |\nabla u|^2 dS$$

$$u|_{\partial u_0} = \alpha_0, u|_{\partial u_1} = \alpha_1, u|\partial u_2 = \alpha_2 \tag{4}$$

It can be proved [1] that u is the minimizer of the Dirichlet functional, if for each vertex $\Sigma \backslash (\sigma_0 \cup \sigma_1 \cup \sigma_2)$,

$$\sum_{W \in \Sigma \backslash (\sigma_0 \cup \sigma_1 \cup \sigma_2)} D_{VW} u_W = - \sum_{i=0,1,2} \alpha_i \sum_{W \in \sigma_i} D_{VW} \tag{5}$$

For any pair of vertices V and W, D_{VW} is defined as

$$D_{VW} = \int \int \nabla \phi_V \cdot \nabla \phi_W dS \tag{6}$$

It is easy to see that $D_{VW} = 0$ unless V and W are connected by an edge in the triangulation. As shown in [1], we suppose VW is an edge belonging to two triangles VWX and VWY. From the theory of finite element methods, we know that for $V \neq W$

$$D_{VW} = -\frac{1}{2}(\cot \angle X + \cot \angle Y) \tag{7}$$

where $\angle X$ is the angle at the vertex X in the triangle VWX and $\angle Y$ is the angle at the vertex Y in the triangle VWY

$$D_{VV} = -\sum_{W \neq V} D_{VW} \tag{8}$$

The computation for v, is similar to that of u, using the boundary conditions obtained from (1) derived from the Cauchy-Riemann equations.

5. COMPUTER SIMULATIONS

We tested our algorithm on a data set provided by the Surgical Planning Lab of Brigham and Women's Hospital. The data set is a $256 \times 256 \times 47$ MRA brain image.

First, using the segmentation method of [2, 8] we found the surface of the vessel. We then used the Visualization Toolkit [11] to generate a triangulation of the surface, which was smoothed by using a version of the mean curvature flow. The triangles making up the ends of the tubular surface were removed to produce an open-ended tube.

Next, as described in Section 3, we generated the (thinned, pruned) skeleton for the vessel and then partitioned it and assigned values for the end points. By using this partitioned skeleton as a reference, we obtained several sections of Y-shaped vessels. (In this example, we partitioned the original vessel into three Y-shaped sections.)

Then, as described in the previous section, for each segment of the vessel, we solved the Dirichlet problem for u, which is the real part of the conformal flattening function. We then found the branch point where the gradient is zero and defined a cut as in Section 2. The boundary values of the conjugate function v were obtained by (1) according to the Cauchy-Riemann equations. We then solved for v, which is the imaginary part of the mapping function. Hence, we could conformally flatten the resulting cut surface onto a polygonal region of the plane. The mapping results of all segments were put together to give a global view of the vessel surface. Some of the segments were shifted in the vertical direction to give a better visualization.

We calculated the mean curvature and Gaussian curvature on each point of the surface. The points on the vessel surface were then painted according to the corresponding curvature. We applied the same colors to the flattened image on the plane. This gave a way to visualize the whole structure of the vessel surface at the same time.

In Figure 3 and 4, we show the triangulated surface of the vessel colored by its mean curvature and Gaussian curvature, respectively. Figures 5 and 6 are the flattened surfaces whose corresponding points have been painted by mean curvature and Gaussian curvature as described before. Although these images show the curvature characteristics, other geometric quantities, such as the thickness of the vessel wall, can also be visualized by this method.

6. CONCLUSIONS

In this note, we presented a high-level procedure for the construction of an angle-preserving flattening map of a multiply branched vessel surface derived from volumetric MRA data. The method is based on conformal geometry and harmonic analysis. We also provided a numerical approximation that finds the mapping based on a finite element method.

While we have successfully mapped a multi-branched vessel system, the mapping function ceases to be continuous in the areas close to the cuts of the vessel (i.e., the common part of two neighbor Y-shaped sections). We intend to remedy this by directly flattening the entire multiply connected structure. There are certain numerical problems with doing this on the triangulated surfaces on which we are working at this point. We are now studying how to circumvent these problems as well as how to apply this methodology to various types of medical imagery for better visualization of structures, e.g., lung nodules detected in CT data.

7. REFERENCES

[1] S. Angenent, S. Haker, A. Tannenbaum, and R. Kikinis, "On the Laplace-Beltrami operator and brain surface flattening," *IEEE Trans. on Medical Imaging*, **18** (1999), pp. 700-711

[2] V. Caselles, R. Kimmel, and G. Sapiro, "Geodesic snakes," *Int. J. Computer Vision*, 1998.

[3] H. Farkas, and I. Kra, *Riemann surfaces*, Springer-Verlag, New York, 1991.

[4] S. Haker, S. Angenent, A. Tannenbaum, and R. Kikinis, "Nondistorting flattening maps and the 3D visualization of colon CT images," *IEEE Trans. on Medical Imaging*, **19**(2000), pp. 665-670.

[5] L. Zhu, S. Haker, and A. Tannenbaum, "Conformal flattening maps for the visualization of vessels," to appear in *Proceedings of SPIE*, San Diego, February 2002.

[6] K. Siddiqi, S. Bouix, A. Tannenbaum, and S. Zucker, "The Hamilton-Jacobi Skeleton," *International Journal of Computer Vision*, to appear, 2002.

[7] T. Hughes, *The finite element method*, Prentice-Hall, New Jersey, 1987.

[8] S. Kichenasamy, P. Olver, A. Tannenbaum, and A. Yezzi, "Conformal curvature flows: from phase transitions to active contours," *Archive Rational Mechanics and Analysis*. **134** (1996), pp. 275-301.

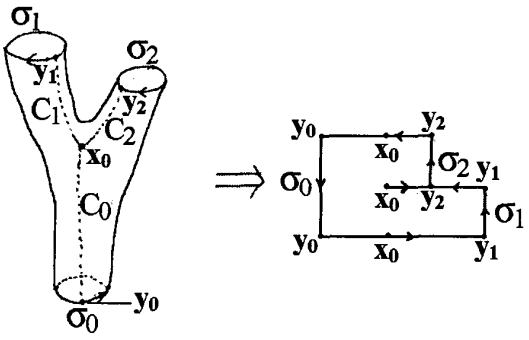

Fig. 1. Mapping a Y-shaped vessel onto the plane.

Fig. 2. The skeleton of a multi-branched vessel

[9] Z. Nehari, *Conformal mapping*, Dover Publications, New York, 1975.

[10] J. Rauch, *Partial differential Equations*, Springer-Verlag, New York, 1991.

[11] W. Schroeder, H. Martin, and B. Lorensen, *The Visualization Toolkit*, Prentice-Hall, New Jersey, 1996.

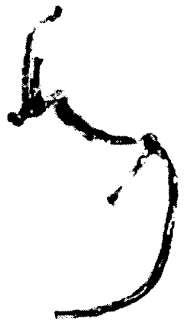

Fig. 3. Mean curvature of the vessel.

Fig. 4. Gaussian curvature of the vessel

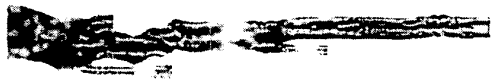

Fig. 5. Points colored according to mean curvature on flattened vessel.

Fig. 6. Points colored according to Gaussian curvature on flattened vessel.